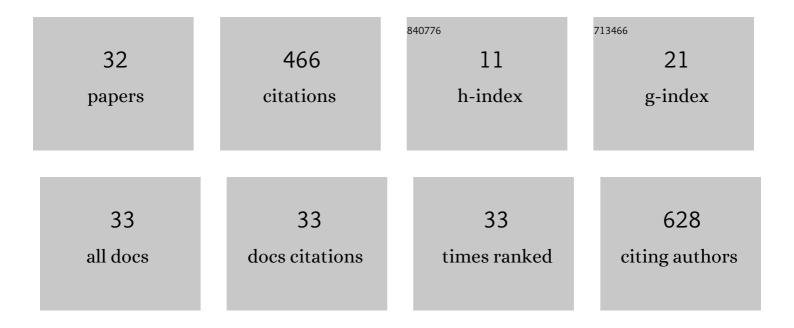
## Matthew L Whitaker

List of Publications by Year in descending order

Source: https://exaly.com/author-pdf/4132660/publications.pdf Version: 2024-02-01



#	Article	IF	CITATIONS
1	The Role of Pressure in Producing Compositional Diversity in Intraplate Basaltic Magmas. Journal of Petrology, 2006, 48, 365-393.	2.8	81
2	Can crystallization of olivine tholeiite give rise to potassic rhyolites?—an experimental investigation. Bulletin of Volcanology, 2008, 70, 417-434.	3.0	77
3	Thermal equation of state of Mg3Al2Si3O12 pyrope garnet up to 19ÂGPa and 1,700ÂK. Physics and Chemistry of Minerals, 2012, 39, 589-598.	0.8	41
4	Elasticity and sound velocities of polycrystalline Mg3Al2(SiO4)3 garnet up to 20 GPa and 1700 K. Journa of Applied Physics, 2012, 112, .	2.5	30
5	Deformation T-Cup: A new multi-anvil apparatus for controlled strain-rate deformation experiments at pressures above 18ÂGPa. Review of Scientific Instruments, 2014, 85, 085103.	1.3	24
6	Melting of the Martian mantle from 1.0 to 4.5 GPa. Journal of Mineralogical and Petrological Sciences, 2013, 108, 201-214.	0.9	23
7	Acoustic velocities and elastic properties of pyrite (FeS2) to 9.6 GPa. Journal of Earth Science (Wuhan,) Tj ETQq1 I	0.78431 3.2	4.rgBT /Ov
8	Thermoelasticity of Â-FeSi to 8 GPa and 1273 K. American Mineralogist, 2009, 94, 1039-1044.	1.9	17
9	Experimental and theoretical studies on the elasticity of molybdenum to 12 GPa. Journal of Applied Physics, 2009, 106, .	2.5	16
10	Spin transition, substitution, and partitioning of iron in lower mantle minerals. Physics of the Earth and Planetary Interiors, 2014, 228, 186-191.	1.9	14
11	An Experimental Investigation of the Relative Strength of the Silica Polymorphs Quartz, Coesite, and Stishovite. Geochemistry, Geophysics, Geosystems, 2019, 20, 1975-1989.	2.5	13
12	Making tissintite: Mimicking meteorites in the multi-anvil. American Mineralogist, 2018, 103, 1516-1519.	1.9	12
13	DIASCoPE: Directly integrated acoustic system combined with pressure experiments—A new method for fast acoustic velocity measurements at high pressure. Review of Scientific Instruments, 2017, 88, 034901.	1.3	11
14	Combined in situ synchrotron X-ray diffraction and ultrasonic interferometry study of ε-FeSi at high pressure. High Pressure Research, 2008, 28, 385-395.	1.2	10
15	Compressional and shear wave velocities of Fe2SiO4 spinel at high pressure and high temperature. High Pressure Research, 2008, 28, 405-413.	1.2	10
16	Thermal equation of state of CalrO3 post-perovskite. Physics and Chemistry of Minerals, 2011, 38, 407-417.	0.8	9
17	In situ ultrasonic velocity measurements across the olivine-spinel transformation in Fe2SiO4. American Mineralogist, 2010, 95, 1000-1005.	1.9	8
18	The phase diagram of NiSi under the conditions of small planetary interiors. Physics of the Earth and Planetary Interiors, 2016, 261, 196-206.	1.9	8

MATTHEW L WHITAKER

#	Article	IF	CITATIONS
19	Ultrasonic Acoustic Velocities During Partial Melting of a Mantle Peridotite KLBâ€1. Journal of Geophysical Research: Solid Earth, 2018, 123, 1252-1261.	3.4	8
20	Spin transition and substitution of Fe3+ in Al-bearing post-Mg-perovskite. Physics of the Earth and Planetary Interiors, 2013, 217, 31-35.	1.9	6
21	Unconventional high-pressure Raman spectroscopy study of kinetic and peak pressure effects in plagioclase feldspars. Physics and Chemistry of Minerals, 2020, 47, 1.	0.8	6
22	Stress distribution during cold compression of a quartz aggregate using synchrotron Xâ€ray diffraction: Observed yielding, damage, and grain crushing. Journal of Geophysical Research: Solid Earth, 2017, 122, 2724-2735.	3.4	5
23	Bulk modulus of Fe-rich olivines corrected for non-hydrostaticity. Comptes Rendus - Geoscience, 2019, 351, 86-94.	1.2	5
24	Carbon is not required during crystallization to produce ferrobasalts/ferrodiorites (FTP rocks). American Mineralogist, 2007, 92, 1750-1755.	1.9	4
25	The Elastic Properties of β-Mg2SiO4 Containing 0.73 wt.% of H2O to 10 GPa and 600 K by Ultrasonic Interferometry with Synchrotron X-Radiation. Minerals (Basel, Switzerland), 2020, 10, 209.	2.0	4
26	Equation of state and sound wave velocities of fayalite at high pressures and temperatures: implications for the seismic properties of the martian mantle. European Journal of Mineralogy, 2021, 33, 519-535.	1.3	2
27	Initial Acoustoelastic Measurements in Olivine: Investigating the Effect of Stress on <i>P</i> ―and <i>S</i> â€Wave Velocities. Journal of Geophysical Research: Solid Earth, 2021, 126, e2021JB022494.	3.4	2
28	Note: Elastic wave velocity measurement using ultrasonic system with two-reflectors. Review of Scientific Instruments, 2018, 89, 086105.	1.3	1
29	Synthesis of the Candidate Topological Compound Ni <sub>3</sub> Pb <sub>2</sub> . Journal of the American Chemical Society, 2022, 144, 11943-11948.	13.7	1
30	Ultrasonic acoustic wave velocities of neighborite (NaMgF3) across orthorhombic to cubic phase boundary at high P-T. Physics of the Earth and Planetary Interiors, 2018, 283, 38-42.	1.9	0
31	Stress Distribution During Cold Compression of Rocks and Mineral Aggregates Using Synchrotron-based X-Ray Diffraction. Journal of Visualized Experiments, 2018, , .	0.3	0
32	Proton irradiation effects in Molybdenum-Carbide-Graphite composites. Journal of Nuclear Materials, 2021, 553, 153049.	2.7	0